반도체디스플레이기술학회지 제22권 제4호(2023년 12월)
Journal of the Semiconductor & Display Technology, Vol. 22, No. 4. December 2023.

In-situ Process Monitoring Data from 30-Paired Oxide-Nitride Dielectric Stack Deposition for 3D-NAND Memory Fabrication

Min Ho Kim[*], Hyun Ken Park[*] and Sang Jeen Hong[*†]
[*†] Department of Electronic Engineering, Myoungji University

ABSTRACT

The storage capacity of 3D-NAND flash memory has been enhanced by the multi-layer dielectrics. The deposition process has become more challenging due to the tight process margin and the demand for accurate process control. To reduce product costs and ensure successful processes, process diagnosis techniques incorporating artificial intelligence (AI) have been adopted in semiconductor manufacturing. Recently there is a growing interest in process diagnosis, and numerous studies have been conducted in this field. For higher model accuracy, various process and sensor data are required, such as optical emission spectroscopy (OES), quadrupole mass spectrometer (QMS), and equipment control state. Among them, OES is usually used for plasma diagnostic. However, OES data can be distorted by viewport contamination, leading to misunderstandings in plasma diagnosis. This issue is particularly emphasized in multi-dielectric deposition processes, such as oxide and nitride (ON) stack. Thus, it is crucial to understand the potential misunderstandings related to OES data distortion due to viewport contamination. This paper explores the potential for misunderstanding OES data due to data distortion in the ON stack process. It suggests the possibility of excessively evaluating process drift through comparisons with a QMS. This understanding can be utilized to develop diagnostic models and identify the effects of viewport contamination in ON stack processes.

Key Words : ON stack process; semiconductor process; process data; PECVD; deposition

1. Introduction

3D-NAND flash memory structure has been adopted to enhance the storage capacity of flash memory device [1]. The structure demand higher multi-layer dielectric such as oxide and nitride (ON) vertical multi-dielectric stack and it referred to as the ‘ON stack’ [2]. The number of vertical layers in ON stack directly impacts on the amount of memory cells. Therefore, it is important to achieve the higher ON stack to enhance the storage capacity [3]. By the tight process margin, the deposition process has become more challenging, and it require the accurate process control for achieve higher ON stack [4]. To reduce the product cost and successful process, the process diagnosis technics have been studied [5-7]. Recently the Samsung Display Co. Ltd in Korea reported the process improvement achieve through process diagnosis using process data in the etch process [8]. They emphasize that the etch process is controlled much more accurately. The diagnostic technology has traditionally been focused on the etch process, there is a growing recognition of the importance of accurate control in the deposition process. There is an increasing interest in deposition diagnosis, process data will play a crucial role in this regard.

To establish an accurate process/equipment model, it is important to utilize various types of process data such as optical emission spectroscopy (OES), quadrupole mass spectrometer (QMS), and equipment states [9]. However, adopting plasma diagnosis in the deposition process is challenging due to viewport contamination, especially in multi-dielectric processes such as the ON stack process. Contamination on the viewport leads to reflection and

[†]E-mail: samhong@mju.ac.kr

absorption of light, it is varying for each wavelength. Short-range wavelengths have the potential for more severe reflection on the contaminated viewport than long-range wavelengths. This variation in the OES spectrum, even when the process is stable, causes the index of the diagnostic model to drift due to data distortion. It hinders the appropriate decision of machine learning models and has the potential for misdiagnosis in the plasma process. This issue is particularly severe in the ON stack process due to the several dielectric layers on the viewport. To address these issues, it is crucial to understand data distortion and its influences in the deposition process. This paper presents the potential for misunderstanding OES-based models due to viewport contamination in the ON stack process. It observes the potential increasing of misdiagnosis depending on the degree of contamination.

2. Sensor Description

This paper using non-invasive external sensors during the ON stack process, with the aim of identifying data variations along the cycle. The positions of the sensors are illustrated in the Fig. 1. The detailed description is provided in the respective sections below.

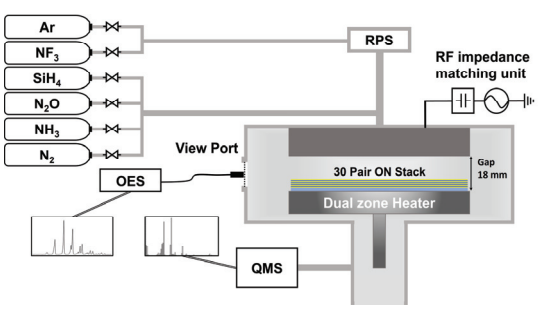

Fig. 1. The schematic of 13.56 MHz CCP PECVD..

2.1 Optical Emission Spectroscopy (OES)

The OES is non-invasive sensor, and it measures the intensity of plasma ray for each wavelength [10]. The each of wavelength corresponds to specific molecular or atomic reaction in the plasma such as excitation, relaxation, ionization, and recombination [11-13]. Which are expressed as spectrum in Fig. 2 [14, 15]. The OES spectrum is collected outside of the chamber and thus, it can't affect to the process result. However, it can be distorted by the viewport contamination. The collected OES data exhibits intensity degradation along the cycle. To ensure a sufficient signal-to-noise ratio for low-intensity peaks, saturated peaks are observed due to the long-integrated time of OES module in the early layer process. The wavelength range of the OES data is from 200 to 1,000 nm, and it measured by OES system with 440 gratings, manufactured by Korea Spectral Products, Seoul, Korea.

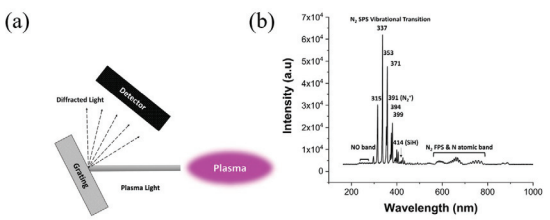

Fig. 2. (a) The schematic of OES measurement and the OES spectrum of 6th oxide layer.

2.2 Quadrupole Mass Spectrometer (QMS)

QMS is also non-invasive external sensor. It measures the current by gas molecules in each of atomic mass unit (AMU) [16]. The each of AMU provides information for gas molecular and fraction of mixture gas and it can be influenced by ionize condition in the process chamber [17]. But it does not represent the information of process chamber due to the different measure position. The QMS data is expressed as spectrum in Fig. 3. The QMS data was measured for the selected AMU (1, 2, 3, 14, 15 … AMU) [18-20]. It was measured using ASTON, a high-sensitivity mass spectrometer, provided by ATIK Co. Ltd, Pangyo, Korea.

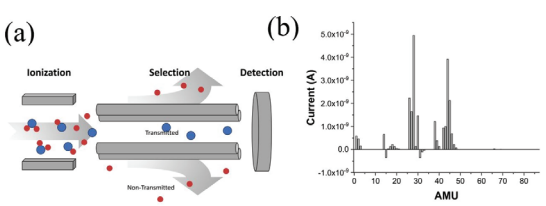

Fig. 3. (a) schematic of QMS measurement and (b) the QMS spectrum of 6th oxide layer.

3. Experiments Methods

The ON stack was deposited using 300 mm PECVD system as shown in Fig. 1. The oxide and nitride layer

vertically stacked and a total of 30 pairs ON stack were deposited over 6 cycles, with 5 pairs of ON stack being deposited in each cycle. The ON stack was deposited using SiH_4 based recipe and it shown in Table 1.

Table 1. The recipe of ON stack process

Parameter	Oxide layer	Nitride layer
Power (W)	400	400
Pressure (mTorr)	2,250	3,500
Temperature (°C)	400	400
Gas Mixture	$SiH_4/N_2O/N_2$	$SiH_4/NH_3/N_2$
Flow Rate (sccm)	200/4,000/3,000	300/1,000/2,500

4. Discussion

In this section, we discuss the risk of misdiagnosis by viewport contamination during the ON stack deposition process. We analysis the potential for misdiagnosis resulting from data distortion, and present two cases for analysis: one involving a reasonable diagnosis using raw data and the potential of misdiagnosis by data distortion. By acknowledging the influence of viewport contamination, we can better understand the implications for reliable process diagnosis.

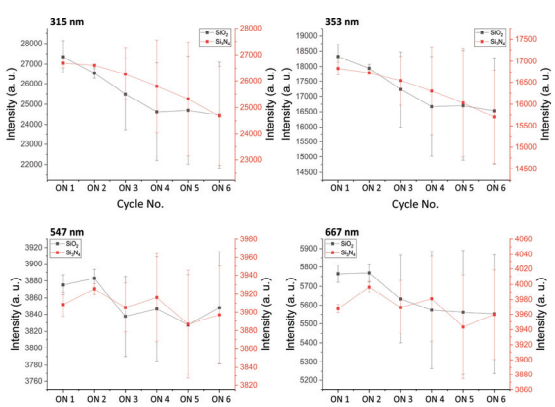

Fig. 4. The trend of OES intensity along the cycle in ON stack process.

The OES and QMS data were analyzed at specific steps in the deposition process, namely at the 2nd, 7th, 12th, 17th, 22nd, and 27th paired oxide steps, which are denoted as ON1, ON2, ON3, ON4, ON5, and ON6, respectively. Fig. 4 shows the trend of OES intensity along the cycle in the ON stack process. we observed the intensity decrease for each wavelength. Especially, it is significant decreased in the shorter wavelengths (below 450 nm) than longer. This decrease can be attributed by ray reflection at the interface layers. Due to the cyclic deposition, multiple interface layers are deposited onto the viewport, and the shorter wavelength ray has much bigger reflectance at the interface layer. Consequently, the short wavelength shows a more significant decrease than longer wavelengths.

Fig. 5 shows the proper diagnosis case using raw data. In Fig. 5 (a), the trend of raw intensity along the deposition cycle is shown. We observed that the SiH peak at 414 nm remains relatively stable, despite the decrease in N_2 related peaks at 405 nm and 660 nm. This implies that wavelengths above 400 nm are less affected by viewport contamination compared to shorter wavelengths. Moreover, the 660 nm peak has a decreasing trend, indicating a decrease in the N_2 gas ratio in the gas mixture. The intensity of the 660 nm peak is related with the N_2 ratio. Fig. 5 (b) presents the corresponding QMS data. To mitigate the effect of data shift, we compared the relative values of H_2 and N_2. The relative value of QMS shows a decreasing trend along the cycle, indicating a change in the gas mixture ratio. Although we cannot quantify the exact amount of change, we believe that the total change in the mixture ratio during the cycle is below 5 %. Because the change of relative value in the ON stack process is less than half compared to the case of a 10 % N_2 decrease in the single oxide process. Furthermore, SiH peaks in the OES data is quite stable. If the N_2 ratio had decreased significantly, we would expect to observe a corresponding change in the SiH intensity. However, since the SiH intensity remains relatively stable, it suggests that the N_2 ratio does not undergo a significant decrease during the ON stack process.

Fig. 6 illustrates the data distortion and a case of misdiagnosis caused by viewport contamination. In Fig. 6 (a), we compared the data variation in the ON stack process and the single oxide process. the single oxide process has same recipe with oxide step in ON stack process and just N_2 flow rate was variated by 10 %. The data from the single oxide deposition process were used as reference data for N_2 ratio change in the process chamber. the OES data from the single oxide deposition process did

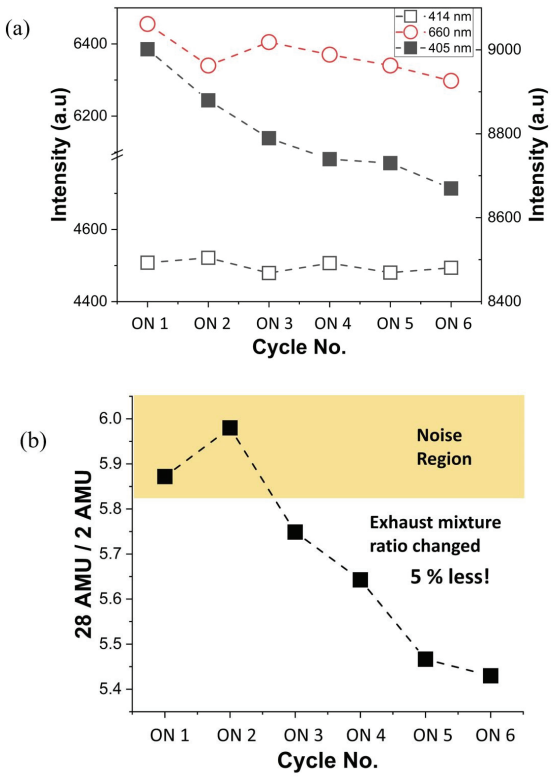

Fig. 5. (a) The trend of selected OES peaks along the deposition cycle and (b) The trend of selected QMS AMU along the cycle.

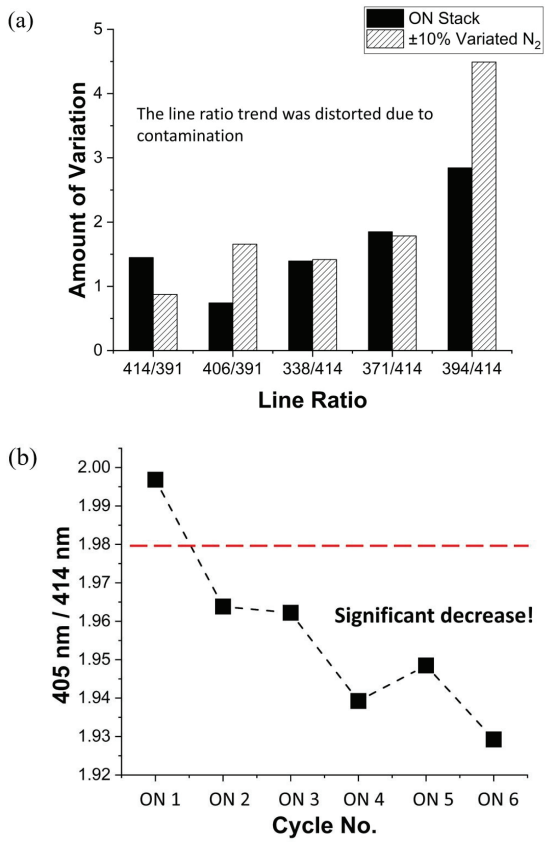

Fig. 6. (a) The amount of variation in selected OES peaks along the deposition cycle and (b) The relative value of OES peaks along the cycle.

not exhibit any data distortion due to viewport contamination. Although the viewport was coated by oxide during the single oxide deposition, this had a negligible effect as the intensity because it did not decrease over the process time. We observed that the ON stack process has less deviation in line ratios compared to the single oxide process. This can be attributed to the significant intensity decrease of shorter wavelengths by contamination. Furthermore, certain line ratios displayed notable variations, such as in the case of ± 10 % N_2 variation. It implies that the viewport contamination can lead to the data distortion, and it can be exaggerating the observed changes beyond their actual magnitude. Fig. 6 (b) shows the case of misdiagnosis with trend of the line ratio in N_2-related peak and SiH. The line ratio in this case is lower than that of the 10 % N_2 decreased case (the value of line ratio 1.98). It implies the severe process drift, and it suggests a gas ratio was changed more than 10 %. But it is not matched with QMS result in Fig. 5. In the case of QMS, it is considered relatively free from viewport contamination by deposition because data is acquired through gas acquisition. We are concluded that the process changes of 5 % less to be relatively reasonable through the results of QMS and the trend of OES raw data. Furthermore, we propose that viewport contamination in the ON stack process has the potential to cause misdiagnosis.

5. Conclusion

To assess the potential for misdiagnosis due to data distortion, we analyzed the raw data from OES and QMS. The conclusion is that OES indicators exhibit changes of over 10% in the gas ratio, whereas RGA indicators show changes of 5% or less in the gas ratio. This difference is attributed to the decrease of OES intensity in short-range

wavelengths, specifically 400 nm and below. As mentioned earlier, the intensity of each wavelength decreases to varying degrees due to the multiple interfaces on the viewport, leading to the distortion of OES data. The intensity decrease is particularly severe in wavelengths of 400 nm and below.

This poses a significant concern for diagnostic techniques, considering that many OES-based diagnostic methods rely on the line ratio method using selected peaks. Such distortions have the potential to undermine the reliability of process diagnosis and increase the risk of misdiagnosis. Therefore, it is crucial to handle OES raw data carefully for accurate process diagnosis in the ON stack process. We emphasize the potential for misdiagnosis when the influence of viewport contamination is ignored.

Acknowledgement

This work was supported by the Technology Innovation Program Development Program-Semiconductor Display Development of Process Technology for Greenhouse Gas Reduction (00155753, GWP 1,000 or Less Chamber Cleaning Gas and its Remote Plasma System for Low GWP Gas) funded By the Ministry of Trade, Industry & Energy (MOTIE, Korea).

References

1. G. H. Lee, S. Hwang, J. Yu and H. Kim, "Architecture and process integration overview of 3D NAND flash technologies," *Applied Sciences*, vol. 11, no. 15, p. 6703, 2021.
2. Y. Li and K. N. Quader, "NAND flash memory: Challenges and opportunities," *Computer*, vol. 46, no. 8, pp. 23-29, 2013.
3. S. Lee, "Technology scaling challenges and opportunities of memory devices," in *Proc. 2016 IEEE IEDM*, San Francisco, CA, USA, 2016, pp. 1-1
4. Y. Yanagihara, K. Miyaji and K. Takeuchi, "Control gate length, spacing and stacked layer number design for 3D-stackable NAND flash memory," in *Proc. 2012 4th IEEE International Memory Workshop*, Milan, Italy, 2012, pp. 1-4.
5. S. H. Kim, C. Y. Kim, D. H. Seol, J. E. Choi and S. J. Hong, "Machine learning-based process-level fault detection and part-level fault classification in semiconductor etch equipment," *IEEE Trans. Semicond. Manuf.*, vol. 35, no. 2, pp. 174-185, 2022.
6. P. Dreyfus, F. Psarommatis, G. May and D. Kiritsis, "Virtual metrology as an approach for product quality estimation in Industry 4.0: a systematic review and integrative conceptual framework," *Int. J Prod. Res.*, vol. 60, no. 2, pp. 742-765, 2022.
7. S. S. Fan, C. Hsu, D. Tsai, F. He and C. Cheng, "Data-driven approach for fault detection and diagnostic in semiconductor manufacturing," *IEEE Transactions on Automation Science and Engineering*, vol. 17, no. 4, pp. 1925-1936, 2020.
8. S. Park, J. Seong, Y. Jang, H. Roh, J. Kwon, J. Lee, S. Ryu, J. Song, K. Roh and Y. Noh, "Plasma information-based virtual metrology (PI-VM) and mass production process control," *Journal of the Korean Physical Society*, vol. 80, no. 8, pp. 647-669, 2022.
9. J. E. Choi and S. J. Hong, "Machine learning-based virtual metrology on film thickness in amorphous carbon layer deposition process," *Measurement: Sensors*, vol. 16, p. 100046, 2021.
10. B. M. Goldberg, T. Hoder and R. Brandenburg, "Electric field determination in transient plasmas: in situ & non-invasive methods," *Plasma Sources Sci. Technol.*, vol. 31, no. 7, p. 073001, 2022.
11. X. Zhu and Y. Pu, "Optical emission spectroscopy in low-temperature plasmas containing argon and nitrogen: determination of the electron temperature and density by the line-ratio method," *J. Phys. D*, vol. 43, no. 40, p. 403001, 2010.
12. H. J. Lee, D. Seo, G. S. May and S. J. Hong, "Use of in-situ optical emission spectroscopy for leak fault detection and classification in plasma etching," *JSTS: Journal of Semiconductor Technology and Science*, vol. 13, no. 4, pp. 395-401, 2013.
13. H. Fatima, M. U. Ullah, S. Ahmad, M. Imran, S. Sajjad, S. Hussain and A. Qayyum, "Spectroscopic evaluation of vibrational temperature and electron density in reduced pressure radio frequency nitrogen plasma," *SN Applied Sciences*, vol. 3, pp. 1-11, 2021.
14. K. Jo and S. J. Hong, "Performance evaluation of RF generators with in-Situ plasma process monitoring sensors," *Journal of Nanoscience and Nanotechnology*, vol. 19, no. 10, pp. 6499-6505, 2019.
15. S. Yokoyama, M. Hirose and Y. Osaka, "Optical Emission Spectroscopy of the SiH_4-NH_3-H_2 Plasma during the Growth of Silicon Nitride," *Japanese Journal*

of Applied Physics, vol. 20, no. 2, p. L117, 1981.
16. G. L. Glish and R. W. Vachet, "The basics of mass spectrometry in the twenty-first century," *Nature Reviews Drug Discovery*, vol. 2, no. 2, pp. 140-150, 2003.
17. A. Ushakov, V. Volynets, S. Jeong, D. Sung, Y. Ihm, J. Woo and M. Han, "Study of fluorocarbon plasma in 60 and 100 MHz capacitively coupled discharges using mass spectrometry," *Journal of Vacuum Science & Technology A: Vacuum, Surfaces, and Films*, vol. 26, no. 5, pp. 1198-1207, 2008.
18. M. J. Kushner, "Plasma chemistry of He/O_2/SiH_4 and He/N_2O/SiH_4 mixtures for remote plasma-activated chemical-vapor deposition of silicon dioxide," *J. Appl. Phys.*, vol. 74, no. 11, pp. 6538-6553, 1993.
19. H. Ohta, A. Nagashima, M. Hori and T. Goto, "Effect of ions and radicals on formation of silicon nitride gate dielectric films using plasma chemical vapor deposition," *J. Appl. Phys.*, vol. 89, no. 9, pp. 5083-5087, 2001.
20. G. Lu, L. L. Tedder and G. W. Rubloff, "Process sensing and metrology in gate oxide growth by rapid thermal chemical vapor deposition from SiH_4 and N_2O," *J. Vac. Sci. Technol. B:Nanotechnol. Microelectron.*, vol. 17, no. 4, pp. 1417-1423, 1999.

접수일: 2023년 11월 9일, 심사일: 2023년 12월 5일,
게재확정일: 2023년 12월 12일